Localized Electrochemistry on a 10 micron spot of a Monolith Large Electrode: An Avenure for Electrochemical Microarray Analysis**

Gaurav Singh, David Moore, Ravi F. Saraf

Chemical and Biomolecular Engineering, University of Nebraska – Lincoln, Lincoln, NE 58516, USA

Supporting Information

1. Comparison of the in-phase and out-phase optical and current response of redox ions

Fig.S1 (a) shows the voltage versus optical response (Δ_A) i.e., total, in-phase and out-phase and Fig.S1 (b) shows voltage versus I_{AC} i.e., total, in-phase and out-phase for 50mM $K_3Fe(CN)_6$. Similarly Fig.S2 (a) shows the voltage versus optical response (Δ_A) i.e., total, in-phase and out-phase and Fig.S2 (b) shows voltage versus I_{AC} i.e., total, in-phase and out-phase for 50mM $Ru(NH_3)_6Cl_3$. Fig.S3 shows the cyclic voltammetry curves for Au electrode for the redox ions.

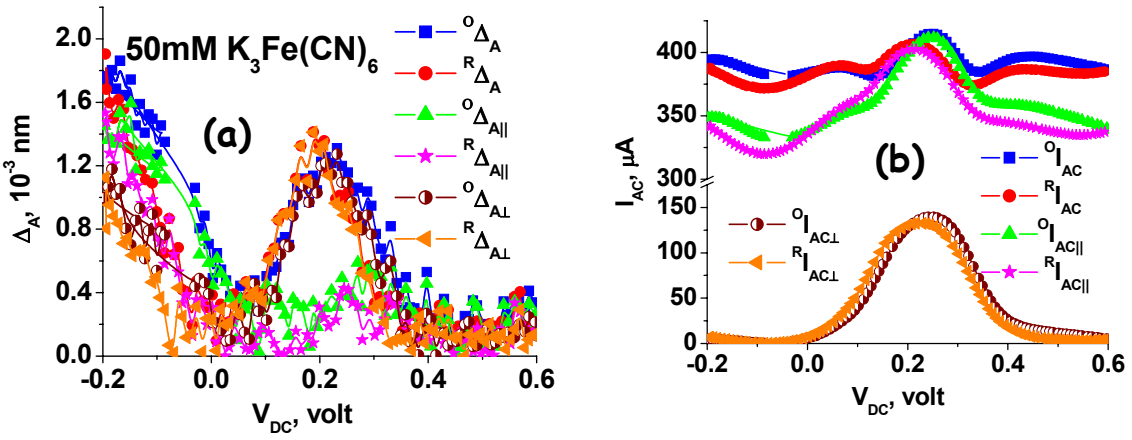

Fig.S1: Optical and AC current signal for potassium ferricyanide

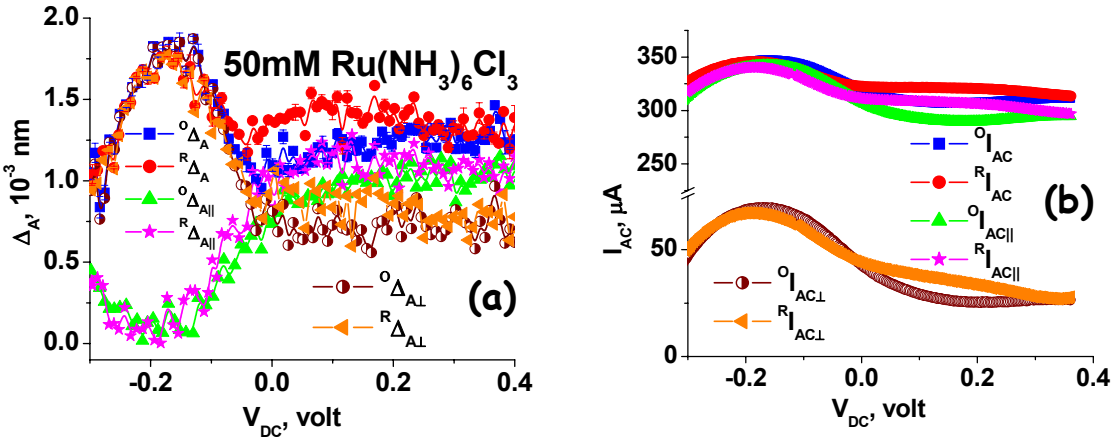

Fig.S2: Optical and AC current signal for hexammine ruthenium trichloride

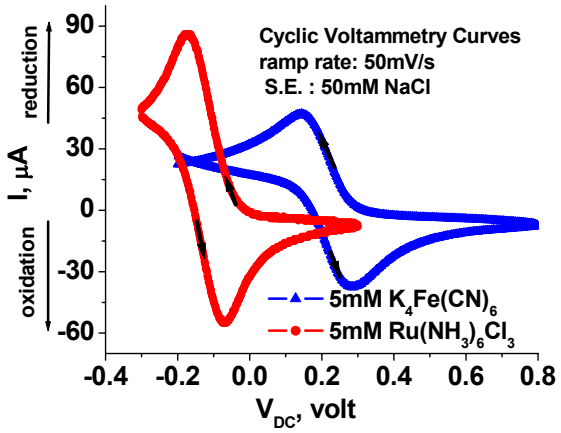

Fig.S3: Cyclic Voltammetry curves for redox couples-potassium ferricyanide and hexammine ruthenium(111) chloride

2. Nanoparticle electrode preparation and measurement

A monolayer of PAH (70K Dalton) was absorbed on clean Au electrode from a 1%(w/w) aqueous solution (immersion time:30min). A drop of citrate coated Au NP (30nm diameter) from Ted Pella Inc. was placed on part of the PAH coated electrode and sealed in a high humidity chamber (to inhibit evaporation) for 24 hours. Subsequently the sample was vigerously washed in DI water to remove excess particles. Fig.S4, shows a composit FESEM image of tow areas of the electrode. In the top portion of the composite image, tow surfaces are observed: the PMMA coated electrode (darker) and the PAH coated Au electrode (lighter). The darker region ate the interface of the tow region is thicker PMMA film due to edge effect caused by dewetting of PMMA. The lower part of the composite image shows three regions: the Au NP coated region (lightest), the PAH coated region (intermediate) and the PMMA region (darkest). Typical region where the lase beam is incident on the sample is shown by a small dotted ellips. The reference spot is on the PMMA region. Fig. 3 compares the interferometric measurement on the two spots indicated in top and bottom composite image in Fig. S4.

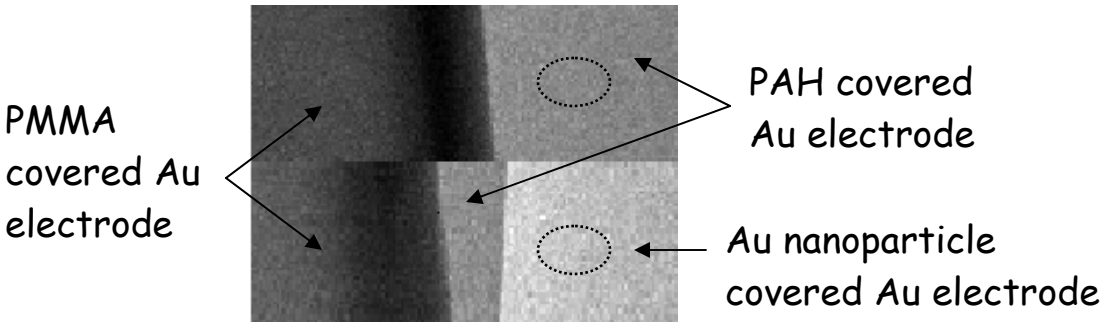

Fig.S4: FESEM (field emission scanning electron microscope) images of measurement config. of Fig.3 to emphasize the ability for combinatorial analysis: the outlined circles represent the sample beam spot size on electrode

3. Fabrication of Reference Electrode

Similar to the method used by Gratz et.al[1] we fabricated an Ag/AgCl (3M KCl) electrode with a porous agar gel plug at the end of a commercial plastic pipette tip with ID=0.5mm and length 8mm. A chloridized Ag wire was inserted inside the pipette and after filling the pipette with saturated AgCl and 3M KCl; the pipette was closed with a rubber stopper with an opening for the Ag wire. The R.E. was calibrated against a commercial Ag/AgCl R.E.(Accumet Glass Body Ag/AgCl # 13-620-53) using a potassium ferricyanide solution and was found to be stable for long periods of time(~2 months).

4. Cyclic-voltametry of ssDNA and dsDNA

Fig. S5 compares the CV of I_{DC} measured during the optical measurement. Two observations are apparent: (i) The redox of the MB, which is the dominant signal in the optical measurement is absent in the CV. (ii) Only the $[Fe(CN)_6]^{-3}$ redox is apparent which shows a passivation due to dsDNA formation. Not discussed in the main paper, but the observation has an important implication: The $[Fe(CN)_6]^{-3}$ ion being negatively charged has stronger repulsion form the surface due to the formation of dsDNA (as DNA is negatively charged molecule) leading to lower redox current, i.e., I_{DC}. Thus, the reduction of Fe^{+3} to Fe^{+2} is more dominant in the ssDNA as apparent from the peak at ~0.18V in Fig. 4. For MB, because the redox is only possible due to "molecular wiring", for ssDNA it is not observed in both optical signal (Fig. 4) and CV (Fig. S5). However, for dsDNA, due to "molecular wiring" the redox of MB must occur – in the CV (Fig. S5) the signal is too low due to 10^3 fold lower concentration compared to $[Fe(CN)_6]^{-3}$; however for the optical signal the discharge is sufficient to lead to a strong signal. The latter is another indication of the high sensitivity of the optical method compared to electrochemical method.

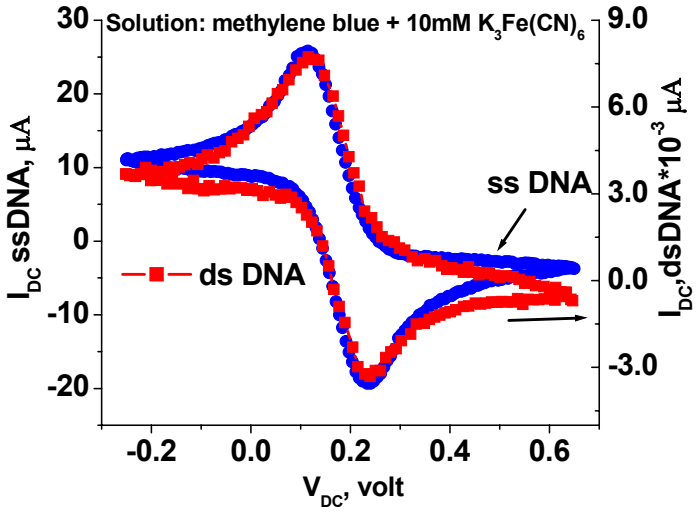

Fig. S5: The CV measured concomitantly with the optical measurements shown in Fig. 4.

5. Optical response due to non-specific binding

Non-specific binding to the immobilized ssDNA is obtained by exposing the monolayer to the same ssDNA sequence (without the terminal groups) followed by ginger washing. Fig. S5 compares the optical response before and after the non-specific binding. Although the noise level is high, the slight reduction in peak due to Fe^{+3} to Fe^{+2} after the non-specific binding is attributed to passivation caused by larger coverage of ssDNA.

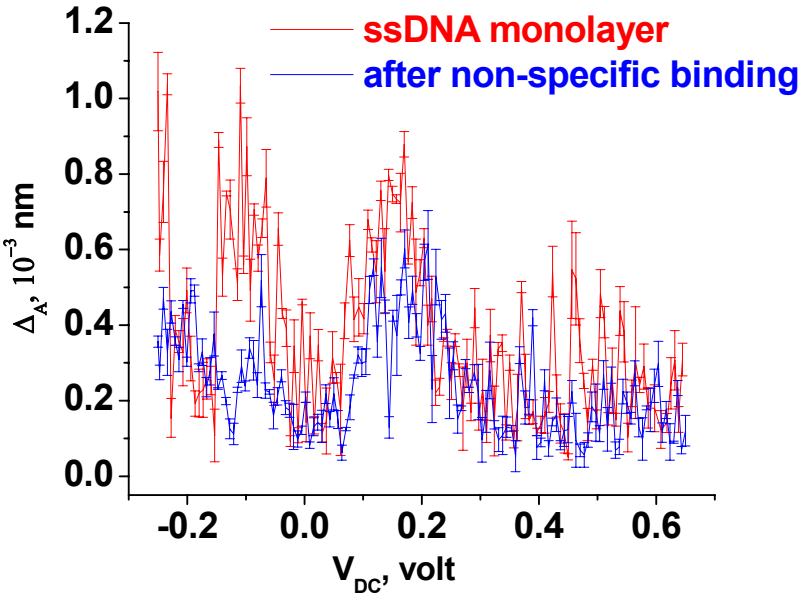

Fig. S5:

Optical response of ssDNA before and after non-specific binding.

References

1. Kashyap, R.; Gratzl, M. *Analytical Chemistry* 1998, *70*, 1468-76.